KINETIC STUDY OF DISSOCIATION OF A COPPER(II) COMPLEX OF A 14-MEMBERED TETRAAZA-MACROCYCLIC LIGAND CONTAINING PYRIDINE AND PENDANT *N*-CARBOXYMETHYL ARMS

Přemysl LUBAL[a,b,*], Anne-Marie ALBRECHT-GARY[b1], Sylvie BLANC[c], Judite COSTA[d,e] and Rita DELGADO[d1,f,*]

[a] *Department of Chemistry, Faculty of Science, Masaryk University, Kotlářská 2, 611 37 Brno, Czech Republic; e-mail: lubal@chemi.muni.cz*

[b] *Laboratoire de Physico-Chimie Bioinorganique, UMR 7509 CNRS, ECPM, 25, rue Bequerel, 67200 Strasbourg, France; e-mail: [1] amalbre@chimie.u-strasbg.fr*

[c] *Laboratoire de Chimie Theorique et Physico-Chimie Moleculaire, UMR 5624 CNRS, Université de Pau et des Pays de l'Adour, 2, rue Jules Ferryl, 64000 Pau, France; e-mail: sylvie.blanc@univ-pau.fr*

[d] *Instituto de Tecnologia Química e Biológia, Universidade Nova de Lisboa, Apartado 127, 2781-901 Oeiras, Portugal; e-mail: [1] delgado@itqb.unl.pt*

[e] *Centro de Estudos de Ciencias Farmaceuticas, Faculdade de Farmácia de Lisboa, Av. Prof. Gama Pinto, 1649-003 Lisboa, Portugal; e-mail: juditec@itqb.unl.pt*

[f] *Instituto Superior Técnico, Av. Rovisco Pais, 1049-001 Lisboa, Portugal*

Received November 3, 2006
Accepted February 4, 2008
Published online March 11, 2008

The kinetics of acid-catalyzed dissociation of the copper(II) complex with 7-methyl-3,7,11,17-tetraazabicyclo[11.3.1]heptadeca-1(17),13,15-triene-3,11-diacetic acid ($ac_2Me[14]pyN_4$) at $[H^+]$ = 0.05–0.25 mol l^{-1}, I = 0.25 mol l^{-1} (Na, H)ClO_4, and T = 298.16 K was studied with conventional and stopped-flow UV/VIS spectroscopy. Three steps of consecutive complex reaction were observed. The very fast first and second steps characterized by k_1 = 70 ± 10 and k_2 = 0.23 ± 0.01 l mol^{-1} s^{-1} depend on the H^+ concentration. The third step is very slow, k_3 = (1.08 ± 0.03) × 10^{-3} s^{-1}, and does not depend on the H^+ concentration. Latter rate-determining step involves an isomerisation process forcing the copper(II) ion to leave rapidly the macrocyclic cavity. The reaction mechanism of the complex dissociation has been proposed, taking into account the results obtained for related systems by independent methods: potentiometry, UV/VIS and EPR spectroscopies, X-ray diffraction analysis, and molecular mechanics calculations.

Keywords: Copper(II) complexes; Pendant acetate arms; Tetraaza-macrocyclic ligands; Aza-crown macrocycles; Pyridinylbackbone; Stability constants; Kinetics.

The main interest in metal complexes of tetraaza-macrocycles consists in their envisaged utilization for medicinal purposes, as contrast agents in

doi:10.1135/cccc20080258

magnetic resonance imaging[1], labeled biological substances with metal radioisotopes for diagnostic and therapeutic purposes – metalloradiopharmaceuticals[2], and/or chelating agents for detoxication from heavy metals[3]. In general, the target-specific metalloradiopharmaceuticals involve a biomolecule, a linker, and a bifunctional chelate (BFC) coordinating a metal radionuclide[2a]. As targeting biomolecules, macromolecules, such as monoclonal antibodies or their fragments or small peptides[2] which are conjugated through the linker to the BFC can be used. The nature of the linker is usually modified so that it can tune the pharmacokinetic properties of the BFC [2]. BFCs, mostly macrocyclic ligands that can be attached to the biomolecule, are chosen according to properties of the radionuclides in order to achieve the desired selectivity. The reactivity of the macrocyclic ligand can be tuned by the type and the number of functional groups of the pendant arms (alkyl chains, carboxylate, phosphinate/phosphonate, hydroxy group, etc.). The steric hindrance and acid/base properties of the ligand can be strengthened by some bulky functional groups bound to the macrocyclic ring, without disturbing its complexing properties. In addition, the ring size and the type of donor atoms of the macrocycle have a great influence on the thermodynamic stability of the metal complex formed.

The following criteria help on the choice of potential BFCs for medical applications[4]: high thermodynamic stability (the radioisotope must be efficiently bound for at least 80% within 1 h under ambient conditions, i.e. pH 4–8, temperature 4–37 °C), fast formation kinetics (the complex has to be formed as quickly as possible after injection into the body) and slow dissociation rate (the complex, once formed, must resist to acid or cation-promoted dissociation in vivo under special conditions, such as low pH in the stomach and liver and/or cation concentration in serum ($[Ca^{2+}] = 1.25 \times 10^{-3}$ mol l^{-1}, $[Zn^{2+}] = 1 \times 10^{-3}$ mol l^{-1}). In addition, non-specific binding of the radioisotope to proteins must be prevented in order to protect them against changes in physiological functions.

The isotopes $^{64,67}Cu$, ^{67}Ga, ^{111}In, ^{90}Y, ^{99m}Tc, ^{177}Lu, $^{186,188}Re$, ^{212}Bi, ^{109}Pd, ^{111}Ag, ^{149}Pm, ^{153}Sm, ^{166}Ho are the most employed radionuclides in practice[2,4]. Copper(II) ion is an attractive radioisotope capable of forming very stable complexes. In addition, copper occurs in the form of several useful isotopes for nuclear medicine, although ^{64}Cu and ^{67}Cu are the most frequently used[2]. Both isotopes (^{64}Cu: half-life 12.8 h, β^+ 655 keV, β^- 573 keV, γ 511 keV; ^{67}Cu: half-life 62 h, β^- 577, 484 and 395 keV, γ 93 and 185 keV) can be used in diagnostics (^{64}Cu in positron emission tomography[2,4]) and in radioimmunotherapy; ^{67}Cu for the treatment of small tumors[5]). Several

copper(II)-containing bioconjugates of cyclen and cyclam acetate derivatives passed clinical trials[2,6].

Kaden et al.[7] incorporated for the first time one pyridine unit into a tetraazamacrocyclic backbone; they measured the kinetic parameters of complexation of transition metal ions (Co^{2+}, Ni^{2+}, Cu^{2+}, Zn^{2+}) in comparison with other tetraaza-macrocycles, such as cyclen and cyclam. They have concluded that the introduction of one pyridine nitrogen into the macrocyclic backbone leads to slower formation of the metal complexes[7].

Some of us pursued the work with tetraaza-macrocycles containing one pyridine subunit[8] and also with some of their derivatives featuring N-pendant arms such as acetate[9], methylphosphonate[10a] or methylpyridine[10b]. It was demonstrated that the pyridine subunit in tetraaza-macrocycles decreased the thermodynamic stability of copper(II) complexes. In contrast, the presence of two pendant functional groups such as carboxylate[9] or methylphosphonate[10] slightly increased the stability.

In the present work, we investigate the reaction pathways in acid-promoted dissociation of copper(II) tetraaza-macrocyclic species ($ac_2Me[14]pyN_4$ in our case, see Chart 1). The kinetic study of the copper(II) complexation with $ac_2Me[14]pyN_4$ (H_2L) was also carried out[11]. It was found out that the course of the complexation can be separated into three reaction steps running on time scales that differ by several orders of magnitude. The first and third steps were described as pH-dependent reactions[11]. In addition, the X-ray crystal structure of $[Cu(H_2L)Cl]^+$ (ref.[12]) has shown that copper(II) adopts a trigonal bipyramidal geometry, with two nitrogen and one carboxylate oxygen atoms in the equatorial plane and the pyridine nitrogen and chloride in the apical positions. The structure of the copper(II) complex of an analogous ligand ($[Cu(HL')]^+$)[10a], where the two pendant acetic arms are replaced by two methylphosphonate ones, was described as a square pyramid with the basal plane defined by three nitrogen atoms of the

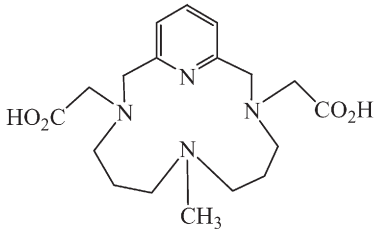

CHART 1
Schematic structure of the macrocyclic ligand $ac_2Me[14]pyN_4$ (H_2L)

macrocyclic framework and one oxygen from a phosphonate group; the apical position was occupied by the nitrogen opposite to the pyridine one. Both structures exhibit comparable copper(II)–nitrogen bonding lengths[10,12]. However, the copper(II)–oxygen bond is longer for the acetate derivative than for the phosphonate one, probably as a consequence of different protonation states of both species.

EXPERIMENTAL

The ligand $ac_2Me[14]pyN_4 \cdot 3HBr \cdot 2H_2O$ was synthesized according to the procedure described in ref.[9a]. A stock solution of copper(II) perchlorate (Merck) was standardized by a complexometric titration with 0.1 mol l^{-1} EDTA (Titriplex Merck), using aqueous 0.1% monosodium salt of 4-(2-pyridylazo)resorcinol as an indicator[13]. Perchloric acid (70%, ®Suprapur Merck) was diluted to the final concentration, 1.0 mol l^{-1}, and standardized with 10^{-1} M sodium hydroxide (®NORMEX, Carlo Erba) using 0.1% phenolphthalein in EtOH as an indicator. All substances were dissolved in deionized distilled water (in the case of NaOH, carbonate-free water was used).

The studied complex [CuL] was prepared by mixing $Cu(ClO_4)_2$ and protonated $ac_2Me[14]pyN_4$ solutions in 1:1 ratio at pH about 3.2, achieved by addition of NaOH for 24 h to ensure the complete complex formation[11]. The acidity of the prepared complex solution was checked with a Tacussel Isis 20 000 pH-meter connected with a high-alkalinity combined electrode (Ingold, U.K.), where the reference electrode consisted of a silver wire coated with silver chloride in a saturated solution of sodium chloride and perchlorate. The analytical electrode was calibrated with five perchloric acid solutions in the concentration range from 1×10^{-4} to 1×10^{-2} mol l^{-1}. The acid-assisted dissociation of the copper(II) complex ($c = 1.04 \times 10^{-4}$ mol l^{-1}) was studied in the 0.05–0.23 mol l^{-1} [H^+] range. The ionic strength of the solutions was adjusted to 0.25 mol l^{-1} with sodium perchlorate ($NaClO_4 \cdot H_2O$; Merck). All experiments were carried out at 298.2 (±0.2) K. The time dependent spectra of copper(II) complex in the time domain of minutes were recorded with a Uvikon 860 (Kontron, Switzerland) equipment, using 1 cm Hellma quartz cuvettes, while the spectra in course of the faster reaction (<100 s) were recorded with a DX 17 MV (Applied Photophysics, U.K.) device equipped with a red filter. The apparent rate constants were calculated with the Biokine program[14] using Laplace–Padé[15a] or simplex[15b] algorithms, having searched for a solution of residual function according to the following condition (*1*)

$$U = \sum_{i=1}^{N} \left[A_{\mathrm{exp},i} - \left(\sum_{j=1}^{3} a_j \, \mathrm{e}^{-k_j t} \right) \right]^2 \rightarrow \min. \qquad (1)$$

The kinetic data were analyzed by the PRO-K-II program[16]. The curve fitting of the experimental points was carried out with the Enzfitter program[17].

RESULTS AND DISCUSSION

The thermodynamic stability of the six-coordinated copper(II) complex of the deprotonated studied macrocyclic ligands H_2L (Scheme 1), [CuL],

slightly increased due to the attachment of pendant acetic arms compared to the parent macrocycle[9]. The optimum experimental conditions for the study of the dissociation kinetics of the complex [CuL] were found from the distribution diagram simulated for I = 0.25 mol l^{-1}. The equilibrium constants (log $K_{p,1}$ = 10.57, log $K_{p,2}$ = 7.67, log $K_{p,3}$ = 4.05, log $K_{p,4}$ = 1.87; log β_{CuL} = 21.32, log β_{CuHL} = 23.60 for I = 0.25 mol l^{-1} (Na,H)ClO_4) were recalculated from the values for I = 0.10 mol l^{-1} (NMe_4NO_3) (log $K_{p,1}$ = 10.72, log $K_{p,2}$ = 7.74, log $K_{p,3}$ = 4.05, log $K_{p,4}$ = 1.8; log β_{CuL} = 21.61, log β_{CuHL} = 23.89), using the extended Debye–Hückel equation, according to SIT [18]. The formation of weak complexes with sodium ions was omitted. The overall distribution diagram for the protonation of the ligand and its copper(II) complexation is given in Fig. 1. Copper(II) forms [CuL] and $H[CuL]^+$ complex species with the studied ligand. The latter complex starts to form at pH ≈ 1 and its formation is complete at relatively high proton concentration (at pH ≈ 2.5, see Fig. 1). Therefore, it is necessary to adjust this H^+ concentration to achieve the complete dissociation of this complex (the working range of $HClO_4$ concentration was 0.05–0.23 mol l^{-1}).

The dissociation kinetics of the copper(II) complex was followed by absorption spectroscopy in the UV region due to a limited amount of ligand, at the maximum of the absorption band of complex (260 nm). An example

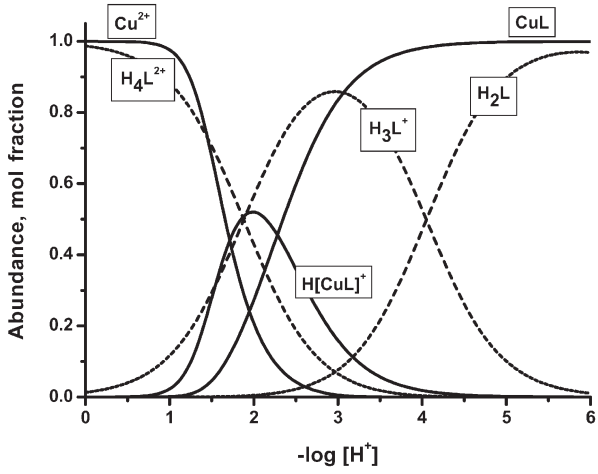

FIG. 1

The distribution diagram for species in the system copper(II)–$ac_2Me[14]pyN_4$, c_{Cu} = 1 × 10^{-4} mol l^{-1}, c_L = 1 × 10^{-4} mol l^{-1}, I = 0.25 mol l^{-1} (Na,H)ClO_4. The equilibrium constants were recalculated from values for ionic strength I = 0.1 mol l^{-1} (NMe_4NO_3)[9]

of kinetic trace of complex dissociation is given in Fig. 2a. As it can be seen, the dissociation of copper(II) complex is complete in about 60 min.

Determination of the number of reaction steps is the most important task in the postulation of the reaction mechanism. Focusing on the start of the chemical reactivity followed by stopped-flow spectroscopy (Fig. 2a, inset), the complex dissociation seems to be a multistep process. The number of reaction steps has been estimated to be equal to three. This hypothesis has been verified by simultaneous global fit of the experimental data obtained from fast and slow scanning equipments by means of the PRO-K-II software

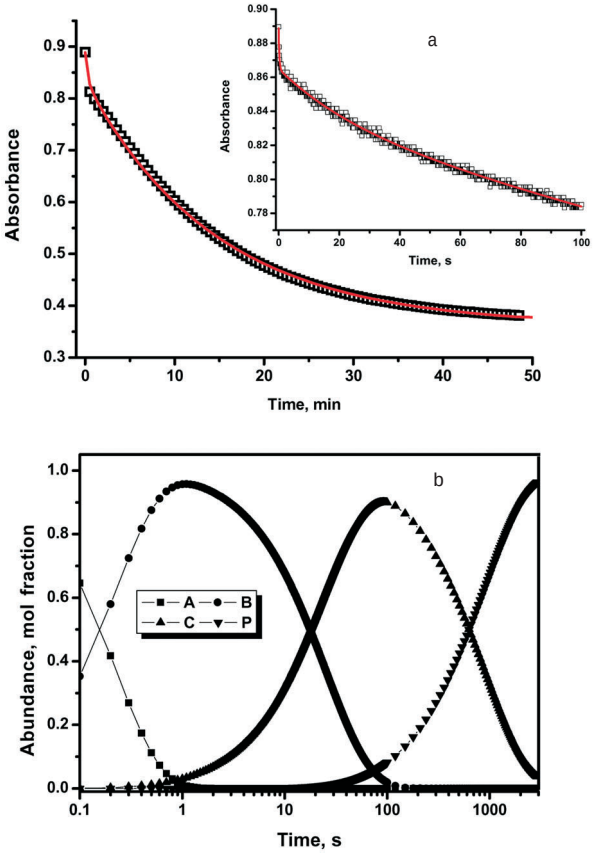

FIG. 2

a Kinetic traces recorded at $\lambda = 260$ nm. $c_{CuL} = 1.04 \times 10^{-4}$ mol l^{-1}, $[H^+]_{tot} = 0.1527$ mol l^{-1}. The experimental points were fitted by three-step kinetic model with the rate constants given in Table I. b The time-distribution diagram calculated for three-step kinetic model with parameters given in Table I. ■ A, ● B, ▲ C, ▼ P

(Table I). Different chemical models concerning consecutive and parallel chemical reactions were tested. As documented by Fig. 2a, the best fit has been obtained for the three-step consecutive mechanism in Scheme 1. In the beginning of the chemical reaction, the first (<1 s) and the second (1 s to 1.5 min) reaction steps are observable by absorbance drop by one tenth (Fig. 2a). The third, slowest step can be followed by a large drop in absorbance to the final value of about 0.35, as a consequence of the presence of protonated ligand species. In addition, the experimental data were treated separately for fast and slow reactions (see Fig. 2b) and the results are comparable (Tables I and II).

$$\mathrm{A} \xrightarrow{k_{1,\mathrm{obs}}} \mathrm{B\ (intermediate\ 1)} \xrightarrow{k_{2,\mathrm{obs}}} \mathrm{C\ (intermediate\ 2)} \xrightarrow{k_{3,\mathrm{obs}}} \mathrm{P}$$

SCHEME 1

The relevant rate laws for the species in Scheme 1 are:

$$\frac{\mathrm{d}[A]}{\mathrm{d}t} = k_{1,\mathrm{obs}}[\mathrm{A}] \qquad (2)$$

TABLE I
Kinetic models obtained by simultaneous global fit of stopped-flow and slowly scanned experimental data[a]. The standard deviations of rate constants are given in parentheses

	Model	Rate constant(s), s^{-1} ε_{260}, $M^{-1}\,cm^{-1}$	Statistical parameters
1.	$\mathrm{A} \xrightarrow{k_{1,\mathrm{obs}}} \mathrm{P}$	$k_{1,\mathrm{obs}} = 1.39_8(1_3) \times 10^{-3}$ $\varepsilon_A = 8150$, $\varepsilon_P = 3671$	$U = 4.760 \times 10^{-2}$ $s(A) = 6.587 \times 10^{-3}$
2.	$\mathrm{A} \xrightarrow{k_{1,\mathrm{obs}}} \mathrm{B\ (Intermediate)}$ $\mathrm{B(Intermediate)} \xrightarrow{k_{3,\mathrm{obs}}} \mathrm{P}$	$k_{1,\mathrm{obs}} = 4.36(9_9) \times 10^{-2}$ $k_{2,\mathrm{obs}} = 1.148(5) \times 10^{-3}$ $\varepsilon_A = 8333$, $\varepsilon_B = 7910$, $\varepsilon_P = 3477$	$U = 4.728 \times 10^{-3}$ $s(A) = 2.078 \times 10^{-3}$
3.	$\mathrm{A} \xrightarrow{k_{1,\mathrm{obs}}} \mathrm{B\ (Intermediate\ 1)}$ $\mathrm{B(Intermediate\ 1)} \xrightarrow{k_{2,\mathrm{obs}}} \mathrm{C(Intermediate\ 2)}$ $\mathrm{C(Intermediate\ 2)} \xrightarrow{k_{3,\mathrm{obs}}} \mathrm{P}$	$k_{1,\mathrm{obs}} = 4.4(5)$ $k_{2,\mathrm{obs}} = 3.97(9) \times 10^{-2}$ $k_{3,\mathrm{obs}} = 1.145(4) \times 10^{-3}$ $\varepsilon_A = 8546$, $\varepsilon_B = 8313$, $\varepsilon_C = 7893$, $\varepsilon_P = 3475$	$U = 3.342 \times 10^{-3}$ $s(A) = 1.748 \times 10^{-3}$

[a] $c_{\mathrm{CuL}} = 1.04 \times 10^{-4}$ mol l^{-1}; $[H^+] = 0.1527$ mol l^{-1}; $I = 0.25$ mol l^{-1} ($NaClO_4$); $T = 298.2$ K.

$$\frac{d[B]}{dt} = k_{1,obs}[A] - k_{2,obs}[B] \quad (3)$$

$$\frac{d[C]}{dt} = k_{2,obs}[B] - k_{3,obs}[C] \quad (4)$$

$$\frac{d[P]}{dt} = k_{3,obs}[C] \quad (5)$$

Applying the mass-balance equation

$$[A]_0 = [A] + [B] + [C] + [P] \quad (6)$$

TABLE II

The observed rate constants determined for the different reaction steps[a]. The standard deviations of rate constants are given in parentheses

$[H^+]$, mol dm^{-3}	$k_{1,obs}$, s^{-1}	$k_{2,obs}/10^{-2}$, s^{-1}	$k_{3,obs}/10^{-3}$, s^{-1} [b]
0.05092	1.12 (5)	2.0 (1)	–
0.05092	1.46 (7)	2.1 (1)	–
0.08144	1.42 (8)	2.08 (1)	–
0.1018	1.7 (1)	2.3 (1)	1.05 (3)
0.1018	1.8 (2)	3.10 (1)	–
0.1222	1.8 (1)	3.0 (1)	–
0.1273	–	–	1.12 (3)
0.1527	4.0 (2)	3.80 (2)	1.11 (3)
0.1527	4.65 (5)	3.4 (1)	–
0.1697	–	–	1.05 (3)
0.1833	5.35 (5)	4.0 (1)	–
0.1867	–	–	1.07 (3)
0.2037	7.71 (7)	4.70 (2)	1.11 (3)
0.2037	–	4.5 (2)	–
0.2206	–	–	1.07 (3)
0.2240	9.5 (1)	5.3 (2)	–
0.2291	–	–	1.05 (3)

[a] $c_{CuL} = 1.04 \times 10^{-4}$ mol l^{-1}; $I = 0.25$ mol l^{-1} ($NaClO_4$); $T = 298.2$ K. [b] Average value $(1.08 \pm 0.03) \times 10^{-3}$ s^{-1}.

the analytical solution of the system of the differential equations (*2*)–(*5*) can be found elsewhere[19].

$$[\mathrm{A}] = [\mathrm{A}]_0 \, \mathrm{e}^{-k_{1,\mathrm{obs}} t} \tag{7}$$

$$[\mathrm{B}] = [\mathrm{A}]_0 \frac{k_{1,\mathrm{obs}}}{k_{2,\mathrm{obs}} - k_{1,\mathrm{obs}}} [\mathrm{e}^{-k_{1,\mathrm{obs}} t} - \mathrm{e}^{-k_{1,\mathrm{obs}} t}] \tag{8}$$

$$[\mathrm{C}] = [\mathrm{A}]_0 \, k_{1,\mathrm{obs}} k_{2,\mathrm{obs}} \left[\frac{\mathrm{e}^{-k_{1,\mathrm{obs}} t}}{(k_{2,\mathrm{obs}} - k_{1,\mathrm{obs}})(k_{3,\mathrm{obs}} - k_{1,\mathrm{obs}})} + \right.$$

$$\left. + \frac{\mathrm{e}^{-k_{2,\mathrm{obs}} t}}{(k_{1,\mathrm{obs}} - k_{2,\mathrm{obs}})(k_{3,\mathrm{obs}} - k_{2,\mathrm{obs}})} + \frac{\mathrm{e}^{-k_{3,\mathrm{obs}} t}}{(k_{1,\mathrm{obs}} - k_{3,\mathrm{obs}})(k_{2,\mathrm{obs}} - k_{3,\mathrm{obs}})} \right] \tag{9}$$

$$[\mathrm{P}] = [\mathrm{A}]_0 \left[1 - \frac{k_{2,\mathrm{obs}} k_{3,\mathrm{obs}} \mathrm{e}^{-k_{1,\mathrm{obs}} t}}{(k_{2,\mathrm{obs}} - k_{1,\mathrm{obs}})(k_{3,\mathrm{obs}} - k_{1,\mathrm{obs}})} - \right.$$

$$\left. - \frac{k_{1,\mathrm{obs}} k_{3,\mathrm{obs}} \mathrm{e}^{-k_{2,\mathrm{obs}} t}}{(k_{1,\mathrm{obs}} - k_{2,\mathrm{obs}})(k_{3,\mathrm{obs}} - k_{2,\mathrm{obs}})} - \frac{k_{1,\mathrm{obs}} k_{2,\mathrm{obs}} \mathrm{e}^{-k_{3,\mathrm{obs}} t}}{(k_{1,\mathrm{obs}} - k_{3,\mathrm{obs}})(k_{2,\mathrm{obs}} - k_{3,\mathrm{obs}})} \right] \tag{10}$$

Equations (*7*)–(*10*) were checked by the MAPLE™ software[20]. Considering that all the reacting species absorb light, the total absorbance at a selected wavelength is defined as

$$A = \varepsilon_A[\mathrm{A}] + \varepsilon_B[\mathrm{B}] + \varepsilon_C[\mathrm{C}] + \varepsilon_P[\mathrm{P}], \tag{11}$$

where ε_A, ε_B, ε_C and ε_P are molar absorption coefficients of all light-absorbing species, which can be obtained simultaneously with the rate constants, using the PRO-K-II software (see Table I). They are in agreement with the following molar absorption coefficients (in l mol^{-1} cm^{-1}, at λ = 260 nm) obtained from the separate treatment of experimental data using Eqs (*7*)–(*11*): ε_P = 3100 ± 300, ε_C = 7100 ± 800, ε_B = 7600 ± 800, ε_A = 7700 ± 800 (the uncertainties were calculated by the propagation of an error method using the MAPLE™ software). The normalized absorption profiles

of all kinetic species present in solution in the course of the dissociation reaction were calculated from both experimental data (Fig. 3). As can be seen, the molar absorptivities of the species A, B and C exhibit shoulders, representing two spectral bands[21]. On the contrary, the product P does not exhibit this diagnostically important shoulder. It was verified numerically that the spectrum of the final product is composed by the contribution of the free protonated ligand species (H_4L^{2+}) having the maximum of absorption band at 260 nm while the copper(II) ion absorbs at lower wavelength region of 240 nm (see Fig. 3). In addition, it can be concluded that all species A, B and C have similar structures.

The acid-assisted dissociation of the copper(II) complex was studied as a function of solution acidity ($[H^+]$ = 0.05–0.23 mol l^{-1}) in order to elucidate the reaction mechanism. All kinetic traces (see Fig. 2a as an example) measured for different proton concentrations were deconvoluted into three steps with the respective observed rate constants (Table II), which were fitted by an empirical function with the H^+ concentration as independent variable. The rate-constant dependences on the H^+ concentration also help to deduce the number of protons involved in the dissociation reaction.

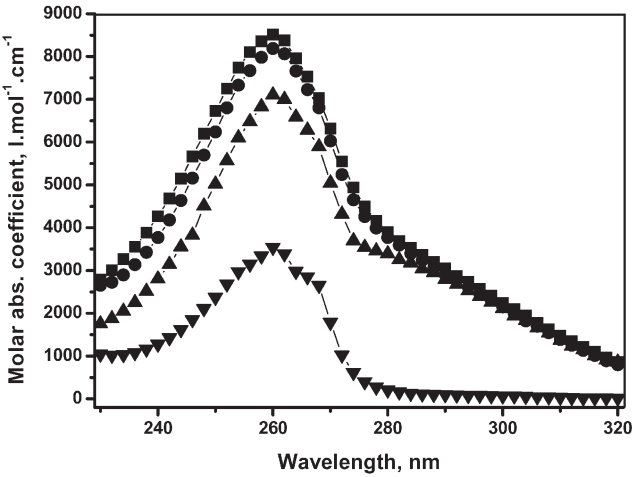

FIG. 3
Calculated molar absorption coefficients ε (in l mol^{-1} cm^{-1}) for thermodynamic and kinetic species. ■ [CuL], ● $H[CuL]^+$, ▲ $[Cu(H_4L)]^{4+}$, ▼ $(H_4L)^{2+}$ + Cu^{2+}

The first observed rate constant can be fitted by the empirical function (Fig. 4)

$$k_{1,\mathrm{obs}} = \frac{a[\mathrm{H}^+]^n}{1 + b[\mathrm{H}^+]} \qquad (12a)$$

and the following parameters were estimated for fixed value b = 190.6 l mol^{-1} (see log K_p(CuL) = 2.28): a = (6.9 ± 0.5) × 10^3 l^2 mol^{-2} s^{-1} (n = 2) and a = (3.7 ± 0.1) × 10^4 l^3 mol^{-3} s^{-1} (n = 3). The number of protons (n) involved in the dissociation reaction of the copper(II) complex was calculated by nonlinear regression as 3.0 ± 0.2 simultaneously with parameter a = (3.7 ± 0.1) × 10^4 l^3 mol^{-3} s^{-1}. Both approaches gave satisfactory results. The best fit was obtained using cubic equation in comparison with quadratic one (see standard deviation of the fit: 0.54 vs 2.70 s^{-1}). In order to improve the fit, another function was applied:

$$k_{1,\mathrm{obs}} = \frac{a[\mathrm{H}^+]^3}{1 + b[\mathrm{H}^+] + c[\mathrm{H}^+]^2} \qquad (12b)$$

which contains the parameters a = (2.0 ± 0.1) × 10^5 l^3 mol^{-3} s^{-1}; b = 510 ± 70 l mol^{-1} and c = (2.8 ± 0.3) × 10^3 l^2 mol^{-2}. However, a worse fit (1 × 10 s^{-1})

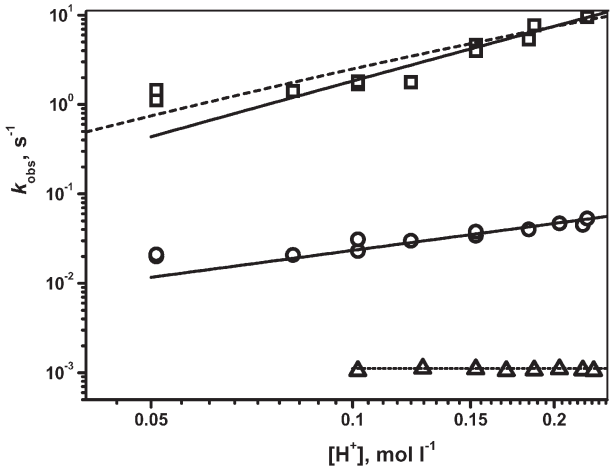

FIG. 4

Dependence of the observed pseudo-first-order rate constants on the acidity of solution for all reaction steps. Calculations using Eqs (*12b*) and (*13*) (full lines) and Eq. (*12a*) (n = 3, dotted lines). The equation parameters are given in the text. □ $k_{1,\mathrm{obs}}$, ○ $k_{2,\mathrm{obs}}$, △ $k_{3,\mathrm{obs}}$

was obtained (see Fig. 4). Therefore, it is concluded that three protons are involved in the first reaction step. This fact indicates that the reaction step has a complex multistep character. Very fast chemical reactions, not detectable with stopped-flow instrumentation, are involved, and the observed reaction step is the slowest one. The second observed rate constant is of the first order with respect to the H^+ concentration (Fig. 4):

$$k_{2,\mathrm{obs}} = d[\mathrm{H}^+] . \qquad (13)$$

The parameter $d = 0.234 \pm 0.009$ l mol^{-1} s^{-1} was calculated. In addition, one H^+ is involved in this reaction step. On the contrary, the third observed rate constant (Table I, Fig. 4) is independent of the H^+ concentration (the reaction order is zero) and, hence, no H^+ takes part in this reaction step. This can be considered as common for acid-assisted dissociation reactions[22,23]. The average value of rate constant $k_{3,\mathrm{obs}} = (1.08 \pm 0.03) \times 10^{-3}$ s^{-1} was calculated. The final products of the complex dissociation from the thermodynamic point of view are Cu(II) and two protonated ligand species, H_4L^{2+} and H_3L^+ (the minor species, see Fig. 1), which was confirmed by comparing their known absorption profiles with the UV/VIS spectrum of the product.

Based on all the above facts, the reaction mechanism has been postulated. As discussed above, the first reaction step involves several reactions:

$$[\mathrm{CuL}] + \mathrm{H}^+ \underset{}{\overset{K_1}{\rightleftharpoons}} \mathrm{H[CuL]}^+ \qquad (I)$$

$$\mathrm{H[CuL]}^+ + \mathrm{H}^+ \overset{K_2}{\rightleftharpoons} \mathrm{H_2[CuL]}^{2+} \qquad (II)$$

$$\mathrm{H_2[CuL]}^+ + \mathrm{H}^+ \xrightarrow{k_1} [\mathrm{Cu(H_3L)}]^{3+} \qquad (III)$$

and the rate of complex dissociation is

$$v = k_{1,\mathrm{obs}}[\mathrm{CuL}]_{\mathrm{tot}} = k_1[\mathrm{H_2CuL}][\mathrm{H}^+] . \qquad (14)$$

Using the mass balance equation together with the definition of protonation constants for the copper(II) complex, one obtains

$$[CuL]_{tot} = [CuL] + [HCuL] + [H_2CuL] =$$

$$= [CuL] (1 + K_1[H^+] + K_1K_2[H^+]^2) . \quad (15)$$

Substitution of Eq. (*15*) into Eq. (*14*) followed by simplification leads to the final relationship:

$$k_{1,obs} = \frac{k_1K_1K_2[H^+]^3}{1+K_1[H^+]+K_1K_2[H^+]^2} . \quad (16)$$

If $1 + K_1[H^+] >> K_1K_2[H^+]^2$, then the former relationship is simplified:

$$k_{1,obs} = \frac{k_1K_1K_2[H^+]^3}{1+K_1[H^+]} . \quad (17)$$

Taking into account $\log K_1 = 2.28$ and the concentration of the acid employed in the study, one suggests that $K_2 << 5$. Both equations are identical to Eqs (*12*) with $a = k_1K_1K_2$, $b = K_1$ and $c = K_1K_2$. Using $a = (3.7 \pm 0.1) \times 10^4$ l^3 mol^{-3} s^{-1} and $b = 190.6$ l mol^{-1} as determined above, the new value $k_1K_2 = 194 \pm 5$ l^2 mol^{-2} s^{-1} was estimated. On the contrary, taking parameters $a = (2.0 \pm 0.1) \times 10^5$ l^3 mol^{-3} s^{-1}, $b = 510 \pm 70$ l mol^{-1} and $c = (2.8 \pm 0.3) \times 10^3$ l^2 mol^{-2}, the new kinetic parameters were calculated: $k_1 = 70 \pm 10$ l mol^{-1} s^{-1}, $K_1 = 510 \pm 70$ l mol^{-1} ($\log K_1 = 2.71 \pm 0.06$), $K_2 = 6 \pm 1$ l mol^{-1} ($\log K_2 = 0.78 \pm 0.07$) and $k_1K_2 = 392 \pm 58$ l^2 mol^{-2} s^{-1}. The calculated value $\log K_1 = 2.71$ is in a good agreement with the value 2.28 found and recalculated from potentiometric data, which supports the hypothesis that both species are identical while the second protonation constant is much lower than the first one, as was predicted. The rate constant k_1 can be considered only as a rough estimate.

The second reaction step can be postulated as

$$[Cu(H_3L)]^{3+} + H^+ \xrightarrow{k_2} [Cu(H_3L)]^{4+} \quad (IV)$$

with the corresponding rate law

$$v = k_1[Cu(H_3L)][H^+] = k_{2,obs}[CuL]_{tot} . \quad (18)$$

Assuming $[CuL]_{tot} = [Cu(H_3L)]$ (see Fig. 2b), one obtains the simplified relationship

$$k_{2,obs} = k_2[H^+] \qquad (19)$$

which is identical to Eq. (*13*) and the parameter is $d = k_2 = 0.234 \pm 0.009$ l mol^{-1} s^{-1}.

The last reaction step is

$$[Cu(H_4L)]^{4+} \xrightarrow{k_3} H_4L^{2+} + Cu^{2+} \qquad (V)$$

and the corresponding rate law is

$$v = k_3[Cu(H_4L)] = k_{3,obs}[CuL]_{tot} . \qquad (20)$$

Defining $[Cu(H_4L)] = [CuL]_{tot}$ (see Fig. 2b), the $k_{obs,3} = k_3 = (1.08 \pm 0.03) \times 10^{-3}$ s^{-1} was obtained. Thus the species in Scheme 1 can be identified as A = $H_2[CuL]^{2+}$, B = $[Cu(H_3L)]^{3+}$, C = $[Cu(H_4L)]^{4+}$ and P = $Cu^{2+} + H_4L^{2+} + H_3L^+$.

For the reaction mechanism proposal, we took into account the single-crystal molecular structures of copper(II) complexes of related macrocyclic ligands[9b,10,12]. An attempt to correlate the structure of copper(II) complexes with spectroscopic properties (mainly molecular UV/VIS and EPR spectra) was in part supported by molecular mechanics calculations[9b,9c]. The copper(II) complex of the diacetato derivative without the methyl group (ac_2[14]pyN_4) exhibits a distorted octahedral structure in trans-conformation, where the four nitrogen atoms of the ring form the equatorial plane and two oxygen atoms of the carboxylate pendant arms are bound in axial positions[9b]. The conformations and lengths of chemical bonds of this structure are similar to a high-temperature isomer of the copper(II) complex of 1,4,8,11-tetraazacyclotetradecane-1,8-bis(methylphosphonic acid) described recently by one of us in refs[24,25]. Taking into account these studies together with the X-ray structures of Co(III) and Ni(II) complexes of the methyl diacetato derivative[9c], it was concluded that [CuL] adopts a structure identical to that of the diacetato derivative without methyl group, i.e., a distorted octahedral geometry in a trans-arrangement[9b,9c]. The trans-(hexacoordinated) and the square-pyramidal (pentacoordinated) conformers of copper(II) complexes have almost the same energy at the average Cu–N distance of 2.06 Å, and both are more stable by 27.2 kJ mol^{-1} than the cis (hexacoordinated) compound[9b,12]. The former complexes are more stable by about 85 kJ mol^{-1} than the trigonal bipyramidal conformer[9c]. Therefore, the rate-determining step for the dissociation of the copper(II) complex of ac_2Me[14]pyN_4 can be explained as the isomerisation process of

the trans or pyramidal conformers to the trigonal bipyramidal one, which is the less favored conformer from the energetic point of view.

Summarizing, the mechanism of the complex dissociation can be established as follows. The copper(II) centre in the [CuL] complex is coordinated by four nitrogen atoms in the equatorial plane and by two axial oxygen atoms. In the first step, two protons are consumed for the protonation of the carboxylate pendant arms (fast steps not detectable by the stopped-flow experiment) followed by the protonation of the nitrogen atom bearing the methyl group. In the second step, the fourth proton is bound to the nitrogen atoms contiguous to the pyridine ring. This is supported by the fact that the rate constant for this process is in rough agreement with the values obtained for acid-promoted decomposition of copper(II) complexes of a new binucleating hexaazapyridinophane ligand described recently[26]. The four-protonated species retain still the trans (square planar) conformation. Therefore, the square planar–trigonal bipyramidal isomerisation process takes place as the slowest reaction step. The trigonal bipyramidal isomer is better accessible to protons than the square planar or the trans conformer. Then the copper(II) ion is released from the macrocyclic cavity, the release being faster than the isomerisation of the complex. This hypothesis is supported also by the fact that the position of the UV absorption maxima of all the kinetic species do not change and their low-energy shoulder (most likely reflecting the Cu–pyridine backbone coordination) does not disappear (see Fig. 3). In addition, the slow reaction step, as a consequence of the isomerisation reaction, was observed during the complexation of copper(II) by the macrocyclic ligand[11]. The high kinetic inertness is due to the good match of the macrocyclic cavity size to the copper(II) centre[9b,9c]. However, the combined isomerisation–dissociation process can be accelerated by the presence of chloride[24]. Of course, some alternative reaction mechanism concerning the complex isomerisation can be proposed.

CONCLUSIONS

The acid-assisted dissociation kinetics of the copper(II) complex with a tetraaza-macrocyclic ligand containing pyridine in the macrocyclic backbone was studied for the first time in detail. This complex dissociation proceeds by three consecutive reaction steps and the respective rate constants have been estimated. The rate-determining step is an isomerisation of the copper(II) complex along which the more stable square-planar conformation is transformed to the less stable trigonal bipyramidal one due to the protonation. These phenomena were also observed for copper(II) complexes

with other macrocyclic ligands[24,25,27]. This detailed study shows that the dissociation of a copper(II) complex of a macrocyclic ligand does have a complex reaction mechanism.

P. Lubal and J. Costa thank the French Ministry of Foreign Affairs for financial support. P. Lubal also acknowledges GRIECES (Portugal) for a travel grant.

REFERENCES

1. a) Botta M.: *Eur. J. Inorg. Chem.* **2000**, 399; b) Aime S., Botta M., Fasano M., Terreno E.: *Acc. Chem. Res.* **1999**, *32*, 941; c) Caravan P., Ellison J. J., Mc Murry T. J., Laufer R. B.: *Chem. Rev.* **1999**, *99*, 2293; d) Aime S., Botta M., Fasano M., Terreno E.: *Chem. Soc. Rev.* **1998**, *27*, 19.
2. a) Liu S., Edwards D. S.: *Bioconjugate Chem.* **2001**, *12*, 7; b) Anderson C. J., Welch M. J.: *Chem. Rev.* **1999**, *99*, 2219; c) Volkert W. A., Hoffmann T. J.: *Chem. Rev.* **1999**, *99*, 2269; d) Reichert D. E., Lewis J. S., Anderson C. J.: *Coord. Chem. Rev.* **1999**, *184*, 3; e) Novak-Hofer I., Schubiger P. A.: *Eur. J. Nucl. Med.* **2002**, *29*, 821.
3. Hancock R. D. in: *Perspectives in Coordination Chemistry* (A. F. Williams, C. Floriani and A. E. Merbach, Eds). Verlag Helvetica Chimica Acta, Basel 1992.
4. a) Parker D.: *Chem. Br.* **1990**, 942; b) Parker D., Morphy J. R., Jankowski K., Cox J.: *Pure Appl. Chem.* **1989**, *61*, 1637.
5. Morphy J. R., Parker D., Kataky R., Eaton M. A. W., Millican A. T., Alexander R., Harrison A., Walker C.: *J. Chem. Soc., Perkin Trans.* **1990**, 573.
6. a) O'Donnell R. T., DeNardo G. L., Kukis D. L., Lamborn K. R., Shen S., Yuan A., Goldstein D. S., Carr C. E., Mirick G. R., DeNardo S. J.: *J. Nucl. Med.* **1999**, *40*, 2014; b) DeNardo S. J., DeNardo G. L., Kukis D. L., Shen S., Kroger L. A., DeNardo D. A., Goldstein D. S., Mirick G. R., Salako Q., Mausner L. F., Srivastava S. C., Meares C. F.: *J. Nucl. Med.* **1999**, *40*, 302; c) O'Donnell R. T., DeNardo G. L., Kukis D. L., Lamborn K. R., Shen S., Yuan A., Goldstein D. S., Carr C. E., Mirick G. R., DeNardo S. J.: *Clin. Cancer Res.* **1999**, *5*, 3330.
7. Schultz-Grunow P., Kaden T. A.: *Helv. Chim. Acta* **1978**, *61*, 2291.
8. Costa J., Delgado R.: *Inorg. Chem.* **1993**, *32*, 5257.
9. a) Costa J., Delgado R., Figueira M. C., Henriques R. T., Teixeira M.: *J. Chem. Soc., Dalton Trans.* **1997**, 65; b) Costa J., Delgado R., Drew M. G. B., Félix V.: *J. Chem. Soc., Dalton Trans.* **1998**, 1063; c) Costa J., Delgado R., Drew M. G. B., Félix V., Henriques R. T., Waerenborgh J. C.: *J. Chem. Soc., Dalton Trans.* **1999**, 3253.
10. a) Guerra K. P., Delgado R., Lima L. M. P., Drew M. G. B., Félix V.: *Dalton Trans.* **2004**, 1812; b) Costa J., Delgado R., Drew M. G. B., Félix V.: *J. Chem. Soc., Dalton Trans.* **1999**, 4331.
11. Perůtka J., Blanc S., Meyer M., Albrecht-Gary A. M., Chaves S., Costa J., Delgado R.: Presented at *Inorganic Reaction Mechanisms Meeting 95, Le Bischenberg, France, January 4–6, 1996*.
12. Alcock N. W., Moore P., Omar H. A. A.: *J. Chem. Soc., Chem. Commun.* **1985**, 1058.
13. Přibil R.: *Analytical Applications of EDTA and Related Compounds*. Pergamon Press, Oxford 1972.

14. *BIOKINE* software. Biologic, Grenoble (France).
15. a) Yeramian E., Claverie C. L.: *Nature* **1987**, *326*, 169; b) Nelder J. A., Mead R.: *Comput. J.* **1965**, *7*, 308.
16. Maeder M., Neuhold Y.-M., Puxty G., King P.: *Phys. Chem. Chem. Phys.* **2003**, *5*, 2836.
17. *ENZFITTER* software. J. Leatherbarrow Edition Biosoft, Cambridge.
18. Grenthe I., Puigdomenech I.: *Modelling in Aquatic Systems*. Nuclear Energy Agency Organization for Economic Co-operation and Development, Paris 1997.
19. Rodiguina N. M., Rodiguina E. N.: *Consecutive Chemical Reactions*. Van Nostrand, Princeton 1964.
20. *MAPLE* version 5.2 for Windows, Waterloo Maple Software. Waterloo University, Waterloo (Canada).
21. Melson G. A. (Ed.): *Coordination Chemistry of Macrocyclic Compounds*. Plenum Press, New York 1979.
22. Wilkins R. G.: *Kinetics and Mechanism of Reactions of Transition Metal Complexes*. VCH, Weinheim 1991.
23. Hay R. W.: *Reaction Mechanisms of Metal Complexes*. Horwood Publishing, Chichester 2000.
24. Kotek J., Lubal P., Hermann P., Císařová I., Lukeš I., Godula T., Svobodová I., Táborský P., Havel J.: *Chem. Eur. J.* **2003**, *9*, 233.
25. Lubal P., Maleček M., Hermann P., Kotek J., Havel J.: *Polyhedron* **2006**, *25*, 1884.
26. a) Diaz P., Basallote M. G., Máñez M. A., Garcia-Espana E., Gil L., Latorre J., Soriano C., Verdejo B., Luis S. V.: *Dalton Trans.* **2003**, 1186; b) Aguilar J., Basallote M. G., Gil L., Hernández J. C., Máñez M. A., Garcia-España E., Soriano C., Verdejo B.: *Dalton Trans.* **2004**, 94.
27. Chen J.-W., Wu D.-S., Chung Ch.-S.: *Inorg. Chem.* **1986**, *25*, 1940.